The United Nations University

GEOTHERMAL TRAINING PROGRAMME
Orkustofnun, Grensásvegur 9,
IS-108 Reykjavík, Iceland

Reports 1999
Number 4

HYDROGEN SULPHIDE DISPERSION MODEL FOR THE MIRAVALLES GEOTHERMAL FIELD, COSTA RICA AND GROUNDWATER FLOW AND CONTAMINANTS TRANSPORT MODELS

Hartman Guido Sequeira
Instituto Costarricense de Electricidad (ICE),
Departamento de Recursos Geotérmicos,
Campo Geotérmico Miravalles,
Bagaces, Guanacaste,
COSTA RICA C.A.

ABSTRACT

In the first part of this report, results of dispersion models of H_2S for the Miravalles geothermal field are presented. Different scenarios are modelled using the available meteorological data for 1999. The programs used for the H_2S dispersion model are the Industrial Source Complex (ISCView) and the Air Force Toxic Dispersion (AFTOX). Results of the simulation show the influence over the towns imparted by H_2S emissions from the power plants Miravalles II, III and I. In the second part, the groundwater and contaminant transport model AQUA3D is studied. Different exercises are presented to show the use of this model in the prediction of groundwater flow and transport of contaminants in the groundwater. These exercises demonstrate the effects of hydrological and geological parameters that will probably be of importance when modelling the wastewater flow from the Miravalles geothermal field.

1. INTRODUCTION

The Miravalles geothermal field is located at the Miravalles volcano in Bagaces Guanacaste between the basins of the rivers Blanco and Cuipilapa. The Miravalles I and II power plants are located at coordinates 298 000N-405 700E at 610 m a.s.l. and the Miravalles III power plant at coordinates 300 150N - 407 050E at 720 m a.s.l. The Miravalles geothermal field is a high-temperature liquid-dominated reservoir with temperature of about 240°C. The proven reservoir area is about 12 km^2, encountered at 700 m depth, and the estimated thickness is between 1000 and 1200 m (Vallejos, 1996). The field is an active hydrothermal area, confined to a caldera-type collapse structure with a diameter of 15 km.

Total dissolved solids in the range of 7000-8000 ppm characterize most of the fluids from the Miravalles geothermal wells, with a pH of about 8 and it is a sodium chloride type water. The non-condensable geothermal gases emitted to the atmosphere are CO_2, H_2S, N_2, CH_4, O_2, H_2, Ar, He, and others in trace quantities. The CO_2 (96-97%), and H_2S (less than 1%) are most important because of possible effects on the environment and human health.

2. THE HYDROGEN SULFIDE DISPERSION MODEL FOR THE MIRAVALLES FIELD

2.1 Introduction

In different environmental impact assessments for Miravalles I, II and III, H_2S emissions were modeled (ICE, 1988 and 1996). The models estimated the concentration of H_2S as under 42 μg/m^3 in the towns, and less than 938 μg/m^3 at 1000 m from the power plants. For the prediction every emission was modeled separately; the effects of all the sources were not considered simultaneously.

In this study, due to the use of more complex programs for the model, the emissions are modeled in a group, which means the model considers the effect of the three power plants simultaneously. This model tries to establish if the power plant emissions can go above the maximum permit limits in populated areas. This limit was established at 42 μg/m^3 in the environmental impact study for Miravalles (ICE, 1996). It is important to underline that 42 μg/m^3 is the limit at which the H_2S is odor perceptible, but not where it poses risk to health.

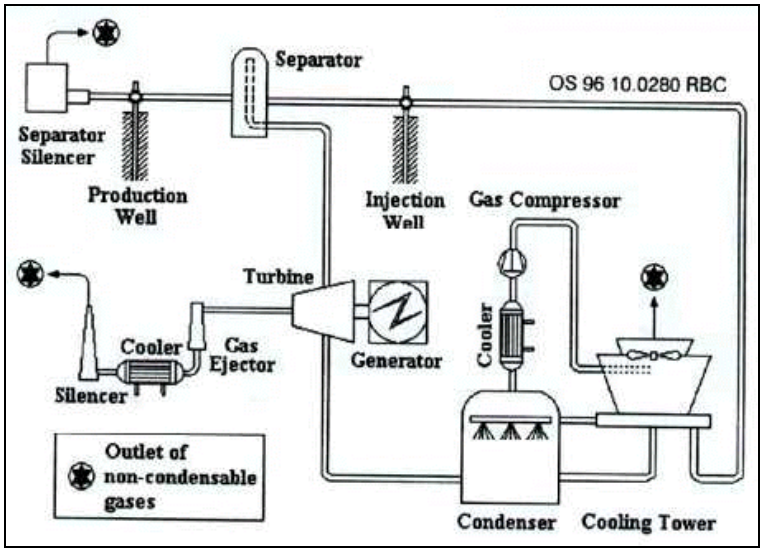

FIGURE 1: Present points of outlet of non-condensible gases in the Miravalles power plants (Bogarin, 1996)

Figure 1 shows the flow of the non-condensable gases from the production wells through the power plant and how they are dispersed to the atmosphere. There are different ways by which the gas can be dispersed to the atmosphere. The gas is released from the silencer when the wells are out of production. In the centrifugal separators the wastewater is sent to injection wells and the steam to the turbine. In the power plant the gas ejector system extracts the non-condensable gases from the turbine condenser. This gas is cooled and discharged to the atmosphere through the cooling tower.

2.2 CO_2 and H_2S

Carbon dioxide (CO_2) is a heavy gas, naturally present in air at concentrations of 0.03-0.06%. It is odourless with an acidic taste. Concentration higher than 5% will produce mental confusion, headache and loss of consciousness; above 10% the loss of consciousness in a few minutes, and at larger concentrations, death due to alteration of blood pH.

CO_2 is also one of the principal greenhouse gases (GHGs). It is estimated that, due to the accumulation of greenhouse gases the global surface temperature will have risen 1.5-3.5˚C by the year 2100 (WHO, 1999a). There are international standards to control the maximum quantities emitted to the atmosphere. This climate change has indirect effects on ecosystems and on the distribution patterns of populations. Table 1 shows some different international standards for CO_2 concentrations.

CO_2 is relatively low in geothermal steam. The emitted level is more environmentally benign than sources such as thermal plants. One important aspect is that the geothermal steam does not contain NOx type gases. In Table 2 there is a comparison between different CO_2 sources.

TABLE 1: Different standards for CO_2 concentrations (Brown, 1995)

Norm	Standard
OSHA	5,000 ppm, 8 hour TWA
NIOSH	10,000 ppm TWA; 30 000 upper limit (10 min)

OSHA: Occupational Safety and Health Administration regulations
NIOSH: National Institute for Occupational Safety and Health recommendations

TABLE 2: Comparison of different CO_2 source emissions (Reed and Renner, 1995)

Emission (kg/MWh)	Geothermal	Coal	Petroleum	Methane
Oxides of Nitrogen (NOx)	0	3.66	1.75	1.93
Carbon Dioxide (CO_2)	0.48	990	839	540

In Miravalles the amount of CO_2 dispersed to the atmosphere is 138 mmol/kg of steam (Bogarin, 1996). The normal concentrations monitored in 1999 in the towns La Fortuna and Guayabo are about 600-700 ppm. Those concentrations are little above natural concentrations in air.

Hydrogen sulfide (H_2S) is a poisonous gas. Like CO_2, it comes from natural sources like volcanic gases, geothermal springs, decaying organic matter and from manmade sources. It is a colourless flammable gas with vapor density of 1.189 and is soluble in water, alcohol, ether and glycerol. The presence of H_2S in the atmosphere increases health risks. Low concentrations can cause human health problems, effects on flora and fauna and damage to man made constructions through corrosion. Higher quantities may cause death. Some countries have strict regulations for maximum emission levels to the atmosphere. Table 3 shows some different international standards for H_2S.

TABLE 3: Different standards for H_2S concentrations

Norm	Standard
TWA PELs OSHA [a]	Acceptable ceiling 28,000 $\mu g/m^3$; 10 minutes maximum ceiling 70,000 $\mu g/m^3$
RELs NIOSH [a]	14,000 $\mu g/m^3$ ceiling 10 minutes of exposures for up to ten hours
ACGIH [a]	14,000 $\mu g/m^3$ for 8 hour average and 40 hour per week to workers
Italy [b]	42 $\mu g/m^3$ as 24 hour averaging time in urban areas
California [c]	42 $\mu g/m^3$ as 1 hour averaging time

[a]Brown, 1995 [b]ICE, 1996 [c]California Air Resources Board, 1999

The human body does not accumulate H_2S. It is excreted in the urine, intestines and expired to the air (Brown, 1995). H_2S smells like rotting eggs and the smell is perceptible in concentrations less than 42 $\mu g/m^3$. When people are exposed to low concentrations of H_2S, it can cause lacrimation, photophobia. Irritation of the nasal mucosa also has a profoundly irritant effect on the cornea producing pain and blurring of vision and keratitis. At 500 $\mu g/m^3$, there is a clearly perceptible odor and the start of damage to some delicate plants. In the range of 280,000 and 700,000 $\mu g/m^3$ it will produce intoxication, and above 840,000 $\mu g/m^3$ it can produce rapid death by asphyxia.

H_2S can contribute to the formation of acid rain. Studies have shown that part of the H_2S emissions from geothermal plants are oxidized in the air to SO_2. The H_2S will oxidize to form elemental sulphur or, ultimately, sulphate (SO_4^{-2}), depending on pH. Oxidation to SO_4^{-2} changes the oxidation state of sulphur ion from –2 to +6.

Corrosion is another important aspect to keep in mind when there is H_2S in the atmosphere. Aluminium conductors in substations and on transmission lines will usually take on a protective coating of black sulphide which inhibits further attack. However, instruments and relay contacts will almost certainly suffer if they feature exposed copper, as sealing is seldom perfect. Contacts and bare connectors of silver are advisable. Exciter commutators of copper can be very troublesome, not only because the copper itself is attacked by H_2S but also because the sulphide film causes sparking at the brushes which wear away at an alarming rate (Armstead, 1983). Table 4 shows the quantities of H_2S emissions for different types of power plants.

TABLE 4: Emanations of H_2S for different types of power plants (Ármannsson and Kristmannsdóttir, 1992)

Type of power plant	Gas emanation (g/kWh)
Coal	11
Oil	11
Gas	0,005
Krafla, Iceland	6
Miravalles	0,41

2.3 Models for gas dispersion in the atmosphere

Gas dispersion models are normally used to predict the impact of pollutant gases in the atmosphere. In this study, the Industrial Source Complex Model (ISC3View) and Air Force Toxic Chemical Dispersion Model (AFTOX) programs are used to predict geothermal H_2S dispersion in the atmosphere.

The Gaussian puff-plume dispersion models are designed for two emission categories i.e. steady-state and instantaneous-state. In the continuous or steady-state, the source emission characteristics are constants in time. In the instantaneous-state the source characteristics do not vary with time but the duration of the emission is limited.

2.3.1 The AFTOX model

AFTOX was designed to model neutrally buoyant gas releases. It is a Gaussian puff-plume dispersion model designed for three emission categories, continuous, instantaneous and finite duration releases (Trinity Consultants, 1999). In the finite duration, the source emission characteristics are constant for several minutes, but in the instantaneous release the emission duration is for only few seconds.

AFTOX uses a Gaussian equation to describe the gas puff dispersion in time. The model assumes that there is no decay nor material deposition. The Gaussian diffusion equation used in the model is

$$G(x,y,z,t-t') = \frac{Q(t')}{2\pi^{3/2}(\sigma_x\sigma_y\sigma_z)}\exp[-\frac{1}{2}(\frac{(x-u(t-t')}{\sigma_x})^2]\exp[-\frac{1}{2}(\frac{y}{\sigma_y})^2]\exp[-\frac{1}{2}(\frac{z-H}{\sigma_z})^2]+\exp[-\frac{1}{2}(\frac{z+H}{\sigma_z})] \quad (1)$$

where G = Concentration in the puff at a given point and time;
Q = Total mass in the puff;
σ_x, σ_y, σ_z = Diffusion parameters like the standard deviation of material concentration in the x, y and z directions; it's assumed that $\sigma_x = \sigma_y$ produces a circular horizontal puff cross-section;
t = Total elapsed time since the spill;

t' = Time of emission of the puff;
u = Wind speed at 10 m elevation;
H = Source height.

If there is an inversion, the expression can be rewritten by adding the following two expressions to the last two terms:

$$\sum \exp[-\frac{1}{2}(\frac{z-H-2NL}{\sigma_z})^2]+\exp[-\frac{1}{2}(\frac{z+H-2NL}{\sigma_z})^2]+\exp[-\frac{1}{2}(\frac{z-H+2NL}{\sigma_z})^2]+\exp[-\frac{1}{2}(\frac{z+H+2NL}{\sigma_z})^2] \quad (2)$$

where L = Mixing layer height;
N = Number of iterations.

When there is a uniformly distributed plume between the surface and the inversion height, the program uses the following equation:

$$G(x,y,z,t-t') = \frac{Q(t')}{2\pi\sigma_x\sigma_y L} \times \exp-\frac{1}{2}[\frac{x-u(t-t')}{\sigma_x}]^2 \times [-\frac{1}{2}(\frac{y}{\sigma_y})^2] \quad (3)$$

At steady-state non-inversion, the following equation is used:

$$C = \frac{Q}{2\pi\sigma_x\sigma_y u} \times \exp[-\frac{1}{2}(\frac{y}{\sigma_y})^2] \times \exp[-\frac{1}{2}(\frac{z-H}{\sigma_z})^2] + \exp[-\frac{1}{2}(\frac{z+H}{\sigma_z})^2] \quad (4)$$

2.3.2 The ISC3View model

Like AFTOX the ISC3View uses an equation to describe the puff dispersion in time. In this case, the model can consider the decay and deposition of material. The following steady-state Gaussian plume equation is used in the model:

$$C = \frac{QKVD}{2\pi u_s\sigma_y\sigma_z} \exp[-\frac{1}{2}(\frac{y}{\sigma_y})^2] \quad (5)$$

where Q = Pollutant emission rate;
K = Coefficient to convert concentration units;
V = Vertical term;
D = Decay term;
σ_x, σ_y = Standard deviation of lateral and vertical concentration distribution in m;
u_s = Wind speed at release height in m/s.

2.3.3 Data used in the Miravalles hydrogen sulfide dispersion model

Both programs need data on meteorological conditions and the source of emission. The meteorological data are used to compute the transport and dispersion of the pollutants.

Emission rates. The amount of H_2S emitted by power plants Miravalles I and II, is estimated at 232.5 tons per year, each (Bogarin, 1996), and for Miravalles III at 60.4 tons per year (ICE, 1996). These values are used in the model.

Modeling area. The main purpose of this study is to predict the concentration of H_2S in the towns. The approximate coordinates for the towns close to the power plants are as follows:

La Fortuna 295000 N - 450000 E;
Cuipilapa 294200 N - 408000 E;
San Pedro 294000 N - 401000 E;
Pueblo Nuevo 301500 N - 400000 E.
Guayabo 298500 N - 402000 E;
San Bernardo 291000 N - 406000 E;
Guayabal 304500 N - 405000 E and

Consequently, the total area selected for the model is between the coordinates 290000-305000 N and 400000-411000 E.

Topographical conditions. The topography and general surface characteristics in the zone are irregular. Using the coefficients given in the programs, the surface roughness lengths are in the range 1.3-0.25 m.

Meteorological data. The models need hourly data on atmospheric conditions at the surface like; temperature, dew point temperature, cloud cover, cloud height, wind speed and direction. The models also need upper air data about height of the mixing layer. In ISC3View the mixing layer height can be estimated using surface data.

The available meteorological data for the model are from the station Casa de Máquinas located at co-ordinates 297800 N-405700 E close to Miravalles I and II power plants. This station collects data on temperature, humidity, precipitation, atmospheric pressure, wind speed and direction. In the models, hourly data for the period between May and August 1999 are used.

Stability parameter. In AFTOX there are several methods to define the stability parameter. The stability may be defined using the Pasquill-Gifford category, the Inverse Monin-Obukhov length or using meteorological conditions. For AFTOX, wind conditions were used to define the stability. Figure 2 shows the wind rose for the Casa de Maquinas station.

In the ISCView program, default parameters established by the Environmental Protection Agency, for considering the atmospheric conditions provided by the meteorological data, are used (EPA, 1999).

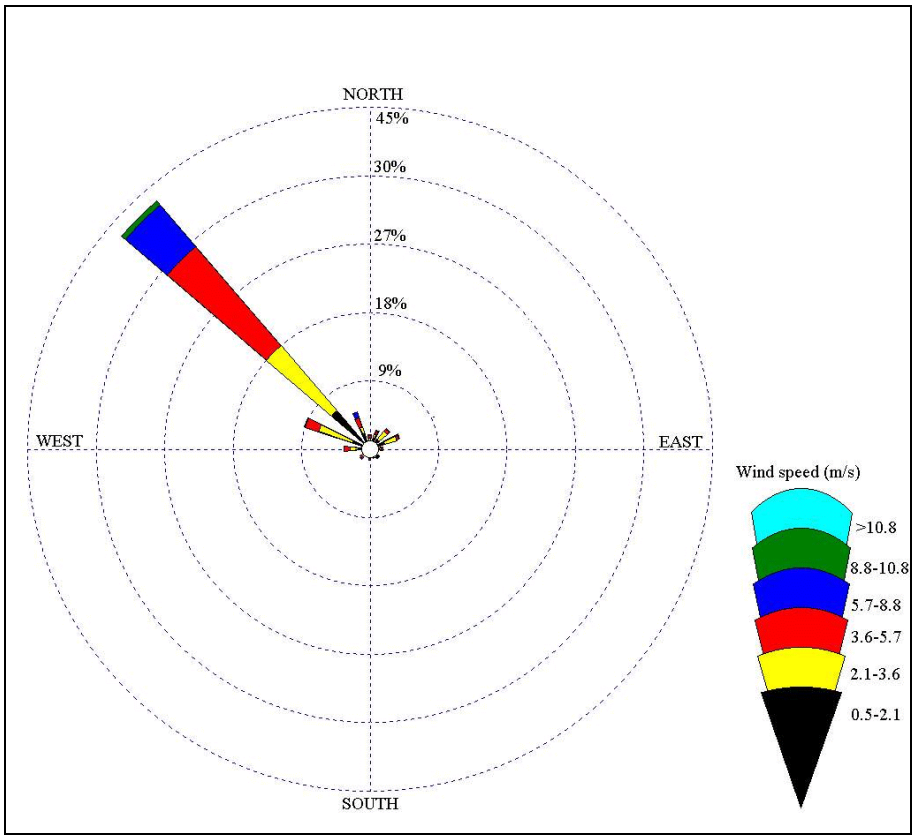

FIGURE 2: Wind rose pattern for Casa de Maquinas station for the period May-August 1999

2.3.4 Results for the Industrial Complex Source (ICSView) model

Currently, only power plants Miravalles I and II are in operation as Miravalles III is under construction. Two different scenarios are modelled using the program ISCView. In the first, the effects of power plants Miravalles I and II only, are modelled. In the second, the effect of power plant Miravalles III has been added.

In Costa Rica the maximum H_2S concentration recommended in towns is 42 µg/m^3 (0.03 ppm) and 938 µg/m^3 (0.67 ppm) at 1000 m from the plant. Both concentrations are one-hour averages. It is important to stress that the World Health Organization (WHO) establishes for workers the limit of 14,000 µg/m^3 (10 ppm) for eight hours of continuous exposure every day for a 40 hour work week without potential risk to health (ICE 1996; WHO, 1999b). Based on these conditions, the model simulated the conditions for averaging time sof one hour and eight hours. But as the results for the eight hours average are very low, it was decided to show rather the results of a simulation of a three hour average which are more conservative.

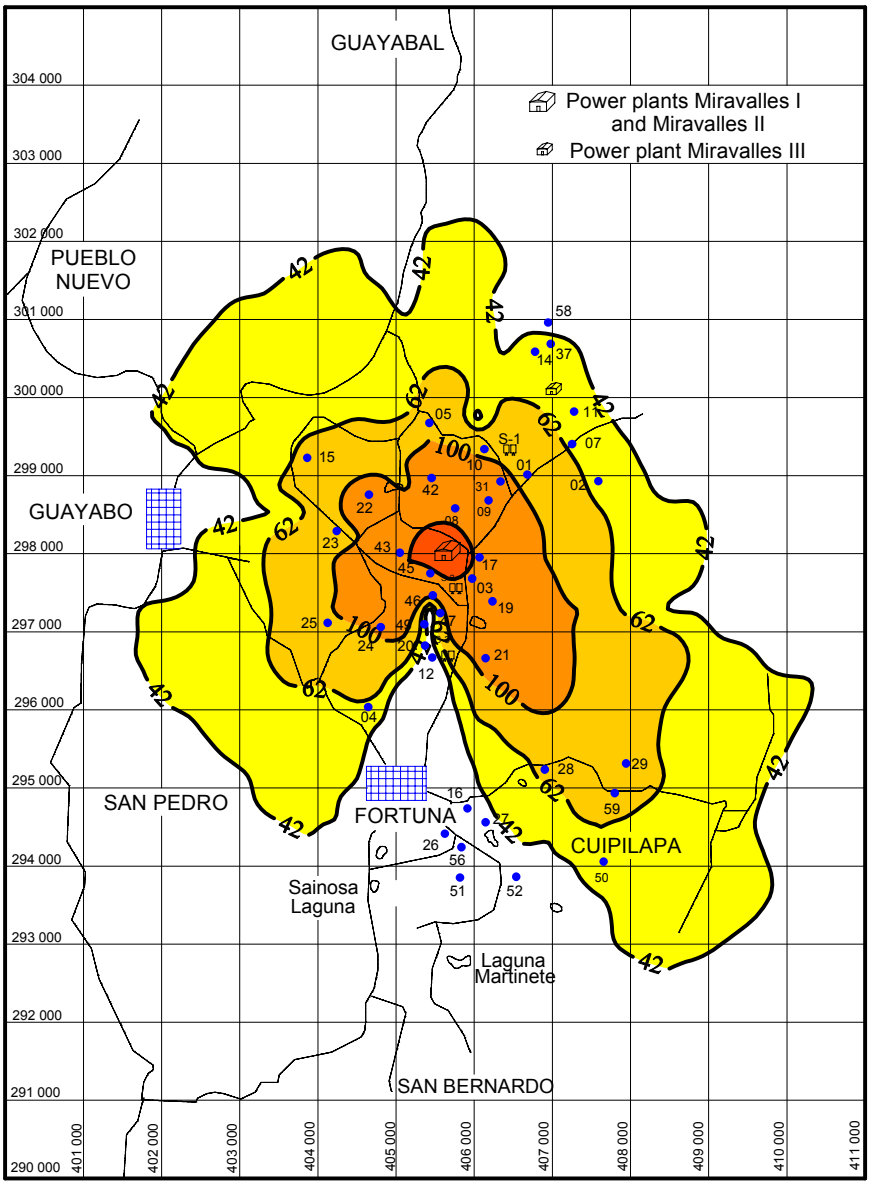

FIGURE 3: ICS H_2S dispersion plume for Miravalles I and II for one-hour average of time

Figures 3 and 4 show the results for the first scenario. Figure 3 presents contours 42, 62, 100 and 442 µg/m^3 (One-hour average). The figures show the effects of wind conditions over plume dispersion. It is possible to establish that the towns Guayabo, La Fortuna and Cuipilapa could at least be subjected to the limit concentration of 42 µg/m^3 under some meteorological conditions. Then it would be necessary to make real measurements of the concentrations of H_2S in these places to determine the real concentrations at the different meteorological conditions. On the other hand, for the simulation of eight-hour averages, the concentration of H_2S near the power plants is below 938 µg/m^3. The maximum value simulated by the model is 1642 µg/m^3 but, as is clear by the contours, such concentrations are reached quite close to the emission source.

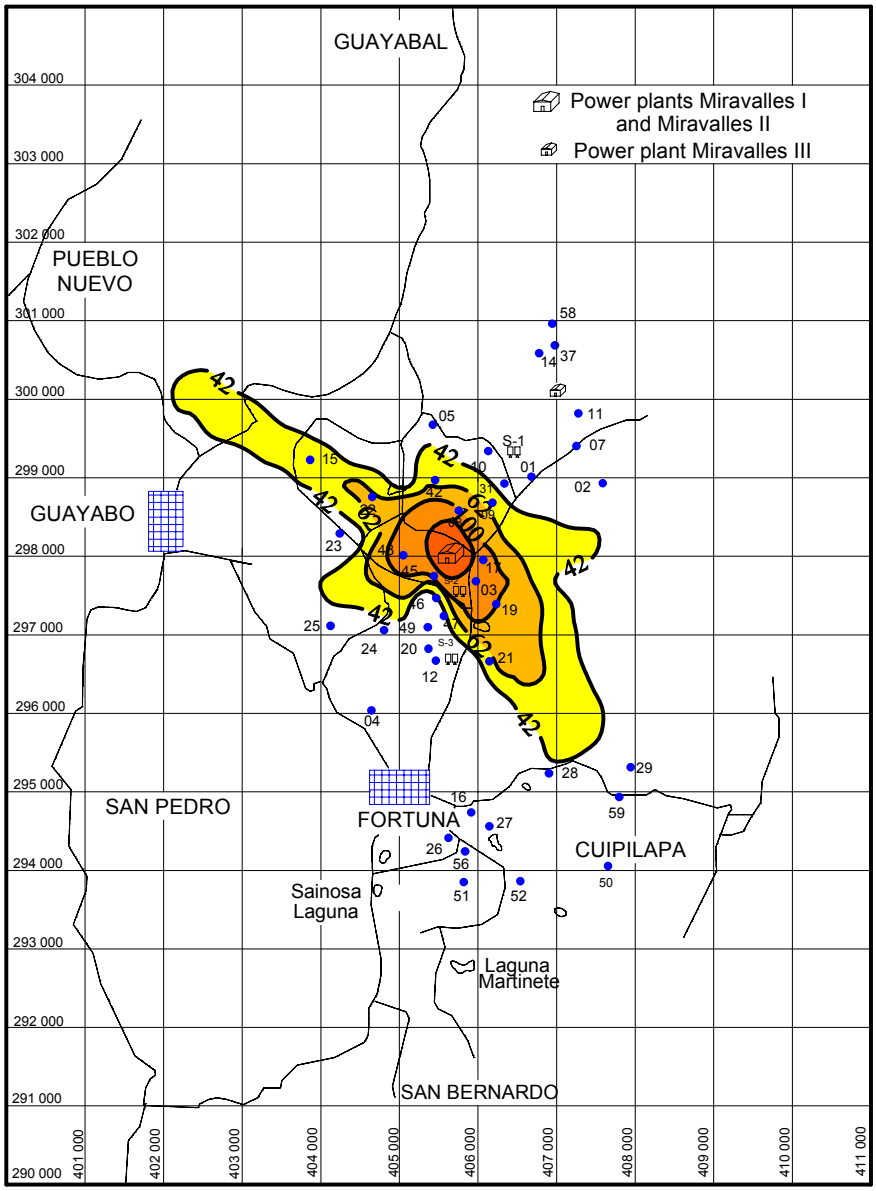

FIGURE 4: ICS H_2S dispersion plume for Miravalles I and II for three-hour average of time

For the simulation of the three-hour average, Figure 4 shows the contours 42, 62, 100 and 200 µg/m^3. In these conditions the effect of the wind direction on the plume are best seen. Now it can be seen that the contour 42 µg/m^3 is shaped along the more frequent wind direction and that the plume distribution does not affect the towns. The maximum concentration of H_2S simulated by the model is 592 µg/m^3 and lower for the one-hour average.

Figures 5 and 6 show the results for the second scenario, when the effect of power plant Miravalles III has been added. Figure 5 shows the one-hour average. The simulation indicates that the affected area is amplified. It means that the possibility of H_2S concentrations close to the value of 42 µg/m^3 in the towns is now substantial. On the other hand, the maximum level obtained is 1642 µg/m^3, the same value as obtained for the first scenario. This means the effect of Miravalles III increases the plume area, but the highest level does not seem to increase and the maximum concentrations do not represent any danger to health or the environment. From Figure 5 it is clear that the major effect of power plant Miravalles III will be to the northeast where there are no densely populated areas, and no impacts.

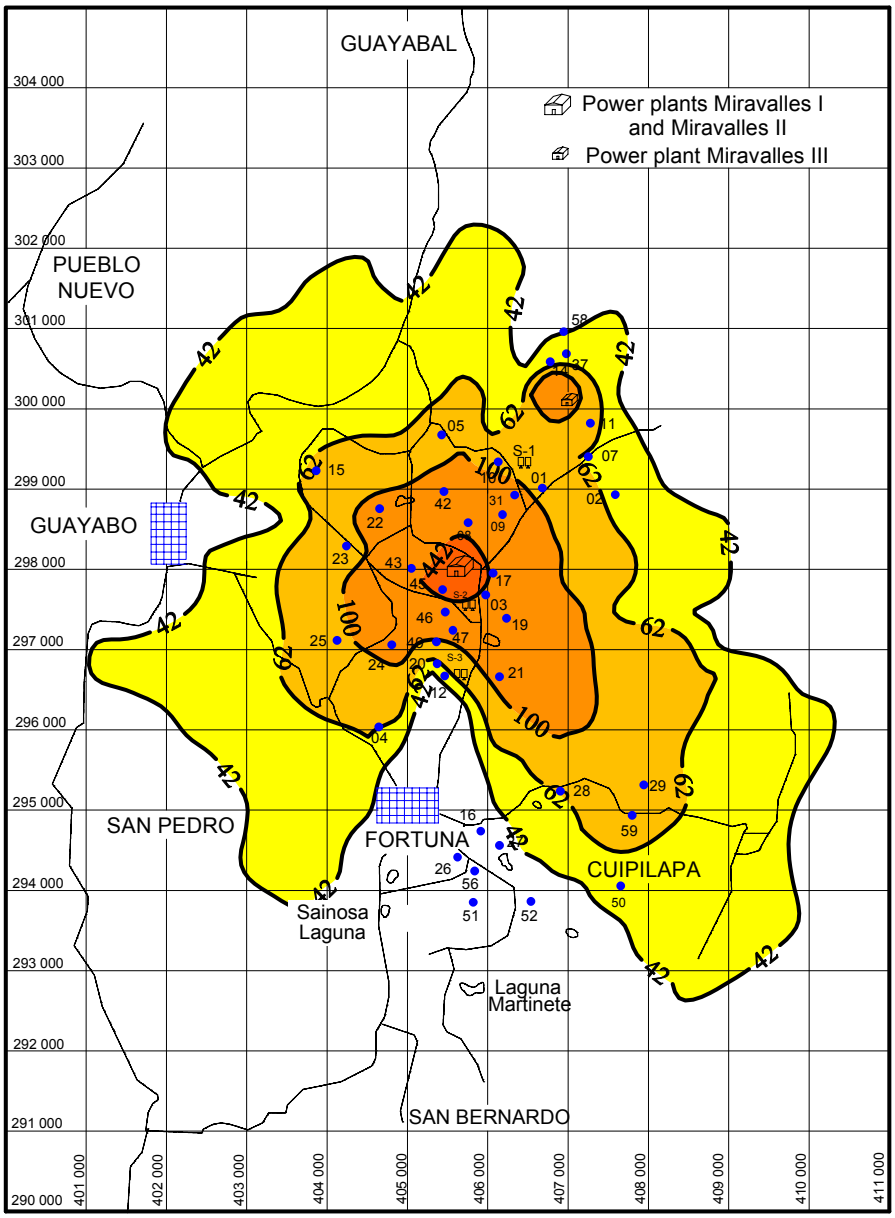

FIGURE 5: ICS H_2S dispersion plume for Miravalles I, II and III for one-hour average in time

Figure 6 shows the simulation for the three-hour average. It is evident that for the three-hour average time, the presence of Miravalles III does not affect the plume dispersion and has only a short range effect close to the emission source. The maximum concentration estimated by the program for these conditions is 592 µg/m^3.

2.3.5 Results for the AFTOX model

AFTOX cannot model more than one emission source and does not consider the meteorological data for periods of time. In AFTOX only one emission point can be modeled at a time and only one type of meteorological condition.

The AFTOX model is based on the Pasquill-Gifford category to define stability class. For the model the more frequent wind conditions are used for the period of study. The standard deviation for the wind direction was used to define the stability class in the zone. For this area, class B (moderately unstable)

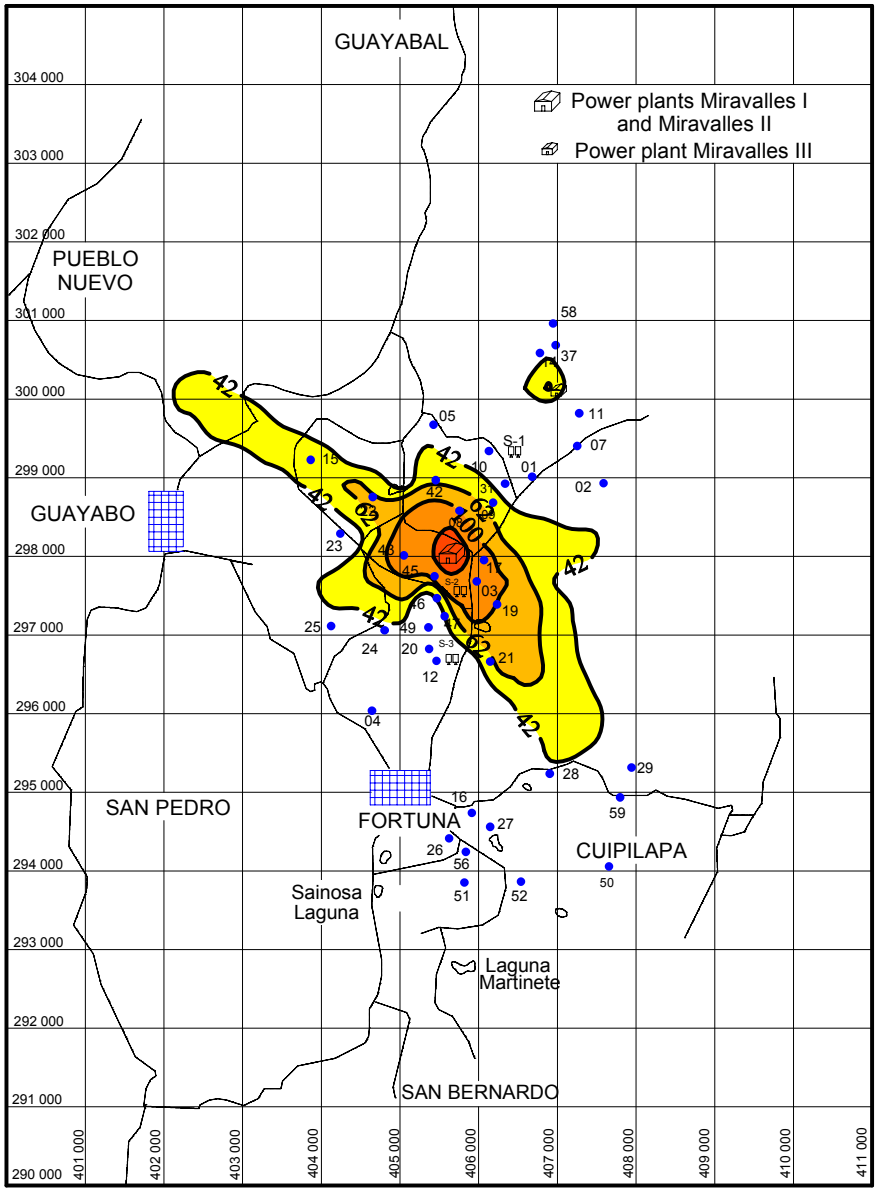

FIGURE 6: ICS H_2S dispersion plume for Miravalles I, II and III for three-hour average in time

and class A (extremely unstable) were used. But to compare the results, class C (Slightly unstable) and class D (neutral stability) were also modelled.

Two average times, one-hour and eight-hours, were modelled. The effects of the emission from the two power plants are modelled as emitting from the same point. That is a very extreme condition because the towers are separated by about 100 m from each other, but gives a good conservative estimate of the effects in the towns.

In Figures 7 and 8, the one-hour average time is presented for different stability and wind speeds. The results are similar to those of ISCView and indicate levels of H_2S lower than 42 $\mu g/m^3$ in the towns. Higher levels are obtained for stability conditions C and D at a low wind speed (1 m/s), i.e. in less frequent conditions. The biggest difference in the concentrations obtained by the ISCView and AFTOX is near to the emission source. The AFTOX model concentrations obtained are higher but that is because the model considers the amount of H_2S from the two power plants as being emitted from the same point.

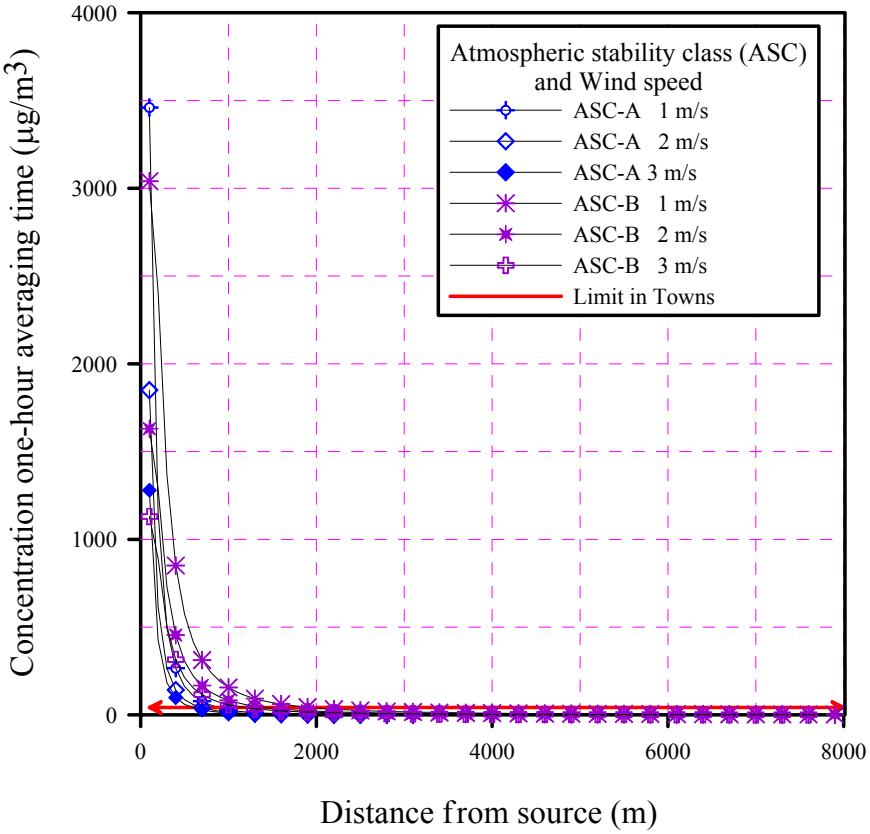

FIGURE 7: AFTOX H_2S dispersion results for Miravalles I, II and III with one-hour averaging time and atmospheric stability classes A and B

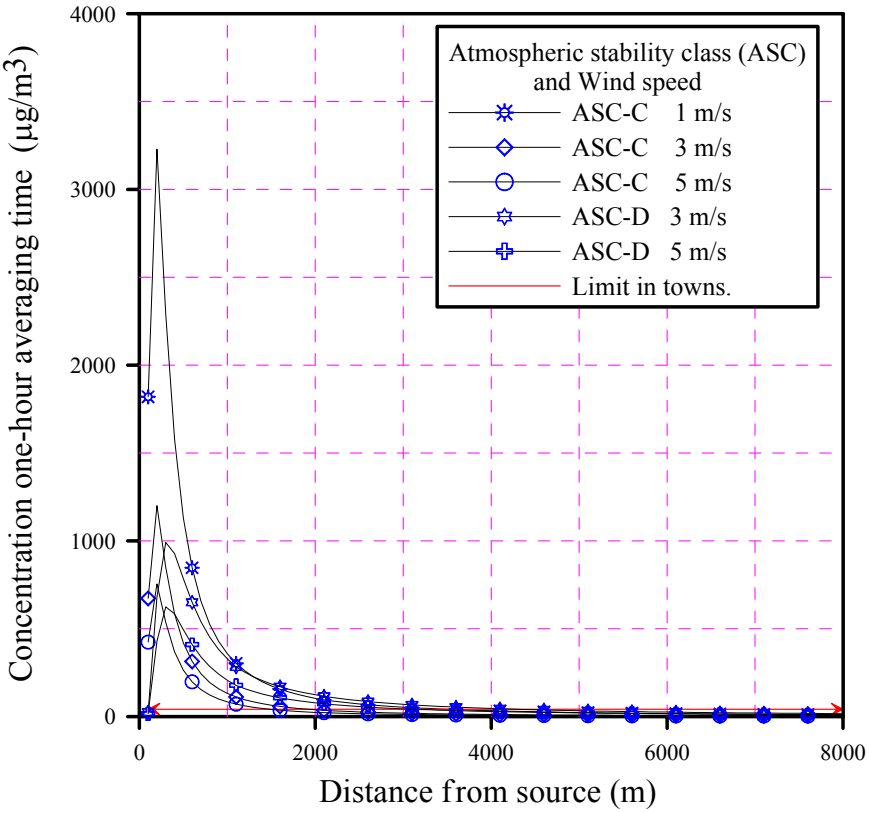

FIGURE 8: AFTOX H_2S dispersion results for Miravalles I, II and III with one-hour averaging time and atmospheric stability classes C and D

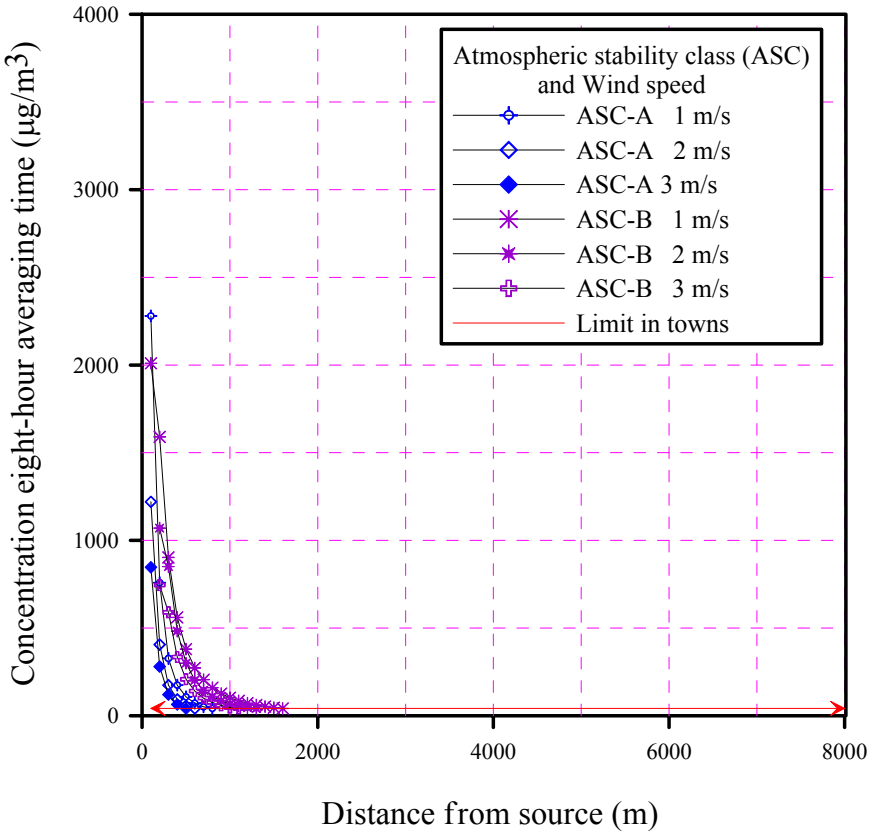

FIGURE 9: AFTOX H_2S dispersion results for Miravalles I, II and III with eight-hour averaging time and atmospheric stability classes A and B

In Figures 9 and 10 the eight-hour average is presented for different stability and wind speeds. Lower concentration of H_2S is calculated and H_2S travels a shorter distance. As in the one-hour average, the longest distances travelled are presented in the stability conditions C and D at low wind speeds (1 m/s).

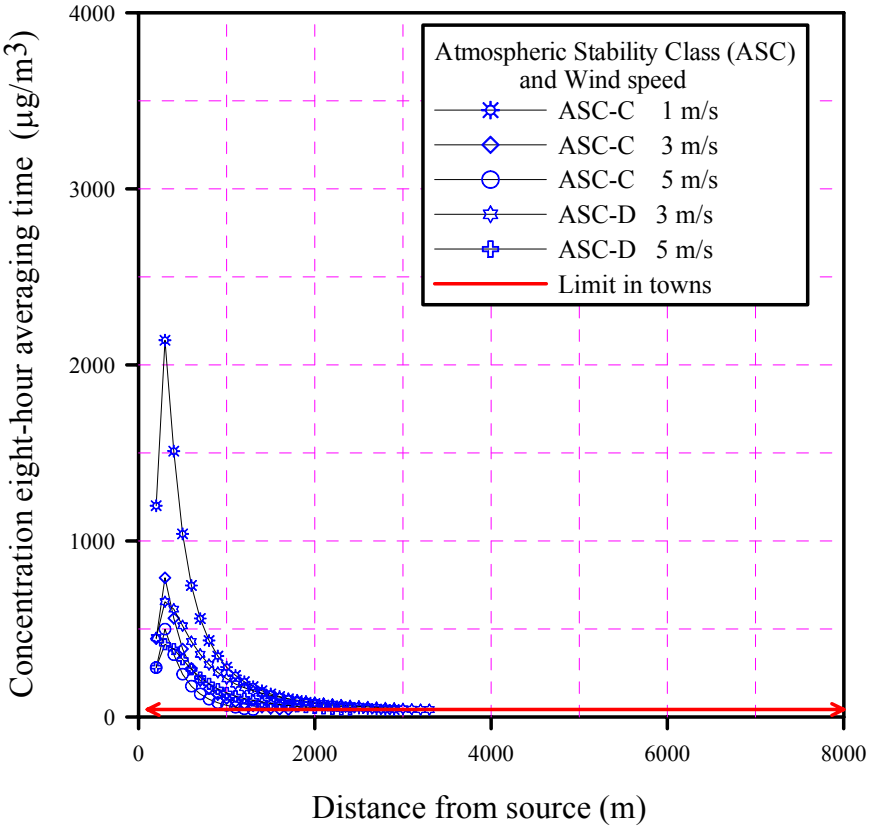

FIGURE 10: AFTOX H_2S dispersion results for Miravalles I, II and III with eight-hour averaging time and atmospheric stability classes C and D

3. WATER POLLUTION AND GROUNDWATER CONTAMINANT TRANSPORT MODEL

The chemical characteristics of Miravalles geothermal water do not allow wastewater disposal into the springs or rivers in the area. In Miravalles, the hot wastewater is re-injected into the reservoir using deep wells. It, therefore, does not represent a pollution problem to the groundwater system. But, in some cases, prior to injection it may be necessary to store the wastewater in surface ponds and due to possible leakages from them, the groundwater can become contaminated. Groundwater models are ideal tools to study and estimate the effect of such leaks. This part of the report describes the AQUA3D groundwater flow and transport model (Vatnaskil, 1998a and 1998b). It was used to study the principles of groundwater flow and distribution of contaminants by setting up hypothetical exercises, which all, one way or another, involve things related to future studies of leakage from ponds in the Miravalles area.

3.1 The AQUA3D model

AQUA3D is a software package developed by Vatnaskil Consulting Engineers to solve 3-dimensional groundwater flow and transport problems using the Galerkin finite element method (Vatnaskil, 1998a and 1998b). AQUA3D solves the equations describing groundwater flow and transport for both homogeneous, isotropic aquifers and inhomogeneous, anisotropic aquifers. To do this, the main hydraulic and hydrogeological features of an aquifer must be defined graphically and mathematically using the software. A model domain is produced which is characterized by tens, hundreds or thousands of individual nodes which are connected by a continuous mesh of triangular elements. The boundary nodes on the external edge (and in some circumstances internal edges) of the model domain are defined by special conditions. These boundary conditions may be prescribed as static or time varying head at a node or a prescribed flow at a node which can vary as a function of time or head. The program also solves the transient transport equations for the movement of contaminants, heat with convection, decay, adsorption and velocity-dependent dispersion. The boundary conditions for transport models can be prescribed concentration or temperature at a node or prescribed dispersive mass flux or heat flux at a node.

3.1.1 Input data for the model

The necessary data for the model includes the following:

Hydrogeological information: The model needs information about the geology such as permeability, anisotropy, porosity, specific yield and dispersion coefficients.

Information about the infiltration into the aquifer as well as the existence of rivers, springs, and wells in the model area.

Real measurement values for water levels and contaminants from a monitoring system that can be used to calibrate the model, that is to adjust the model parameters to within realistic range to fit the measured values. When that is finished the model can be used to predict what will happen in the future.

3.1.2 Description of the flow model

Groundwater flow is governed by Darcy´s law, which in its simplest form can be written as:

$$V = K \times \Delta h \tag{6}$$

where V = Darcy's velocity [m/s];
K = Permeability [m/s];
h = Groundwater head gradient [m].

To describe the three-dimensional groundwater movement, the following equation is used:

$$\frac{\partial}{\partial x}\left(k_{xx}\frac{\partial h}{\partial x}\right)+\frac{\partial}{\partial y}\left(k_{yy}\frac{\partial h}{\partial y}\right)+\frac{\partial}{\partial z}\left(k_{zz}\frac{\partial h}{\partial z}\right)=S_s\frac{\partial h}{\partial t}-Q \qquad (7)$$

where K_{xx}, k_{yy}, k_{zz} = Values of permeabilities along the principal axis [m/s];
h = Piezometric head [m];
Q = Volumetric flux per unit volume [$m^3/s/m^3$];
S_s = Specific storage coefficient [m^{-1}];
t = Time [s].

This equation assumes that the principal axes are in horizontal and vertical planes. The equation applies to a local coordinate system within each element, so anisotropy can vary from element to element.

When several layers are used, the above equation is integrated vertically across each layer and the following equations apply for n different layers.

Top layer:

$$\frac{\partial}{\partial x}\left(k_{xxy}(h_1-zb_1)\frac{\partial h_1}{\partial x}\right)+\frac{\partial}{\partial y}\left(k_{yy}(h_1-zb_1)\frac{\partial h_1}{\partial y}\right)+R+\gamma_2(h_2-h_1)+Q=S_s(h_1-zb_1)\frac{\partial h_1}{\partial t}+S_y\frac{\partial h_1}{\partial t} \qquad (8)$$

Layer *i*:

$$\frac{\partial}{\partial x}\left(k_{xxy}(zt_i-zb_i)\frac{\partial h_i}{\partial x}\right)+\frac{\partial}{\partial y}\left(k_{yy}(zt_i-zb_i)\frac{\partial h_i}{\partial y}\right)+\gamma_i(h_{i-1}-h_i)+\gamma_{i+1}(h_{i+1}-h_i)+Q=S_s(zt_i-zb_i)\frac{\partial h_i}{\partial t} \qquad (9)$$

Bottom layer:

$$\frac{\partial}{\partial x}\left(k_{xxy}(zt_n-zb_n)\frac{\partial h_n}{\partial x}\right)+\frac{\partial}{\partial y}\left(k_{yy}(zt_n-zb_n)\frac{\partial h_n}{\partial y}\right)+\gamma_n(h_{n-1}-h_n)+Q=S_s(zt_n-zb_n)\frac{\partial h_n}{\partial t} \qquad (10)$$

γ_i is the average vertical conductance and is defined as follows:

$$\gamma_i=\frac{1}{\frac{zt_{i-1}-zb_{i-1}}{2k_{zi-1}}+\frac{zt_i-zb_i}{2k_{zi}}+\frac{zb_{i-1}-zt_i}{k_i}} \qquad (11)$$

where S_s = Specific storage coefficient in each layer [m^{-1}];
h_I = Piezometric head in layer i [m];
zb_i = Bottom elevation of layer i [m];
zt_i = Top elevation of layer i [m];
k_{zi} = Vertical permeability in layer i [m/s];
k_i = Vertical permeability in a semi-permeable layer between layer i and i-1 [m/s];
R = Infiltration rate [mm/year];
Q = Pumping injection rate in each layer [m^3/s];
S_y = Specific yield.

The program does not use permeability directly to solve the equations; it uses the permeability to calculate the transmissiviy. The transmissivity or horizontal conductance can be written as follows:

$$\begin{aligned} T_{xx} &= K_{xx} \times \textit{saturated thickness of layer} \\ T_{yy} &= K_{yy} \times \textit{saturated thickness of layer} \end{aligned} \tag{12}$$

The storage coefficients in the top layer and in layer i, respectively, are

$$\begin{aligned} S &= S_s \times \textit{saturated thickness of layer} + S_y \\ S &= S_s \times \textit{saturated thickness of layer} \end{aligned} \tag{13}$$

3.1.3 Description of the transport model

The following equation describes the three-dimensional transport of mass/heat in the groundwater.

$$\begin{aligned} &\frac{\partial}{\partial x}\left(D_{xx}\frac{\partial c}{\partial x}\right) + \frac{\partial}{\partial y}\left(D_{yy}\frac{\partial c}{\partial y}\right) + \frac{\partial}{\partial z}\left(D_{zz}\frac{\partial c}{\partial z}\right) + Q(c_w - c) - \\ &\left(V_x\frac{\partial c}{\partial x} + V_y\frac{\partial c}{\partial y} + V_z\frac{\partial c}{\partial z}\right) = \varphi R_d\frac{\partial c}{\partial t} + \varphi R_d \lambda V_x \frac{\partial c}{\partial x} c \end{aligned} \tag{14}$$

where D_{xx}, D_{yy} and D_{zz} are the dispersion coefficients defined by

$$\varphi D_{xx} = \alpha_L V^n + D_m\varphi \qquad \varphi D_{yy} = \alpha_L V^n + D_m\varphi \qquad \varphi D_{zz} = \alpha_L V^n + D_m\varphi$$

and
- c = Solute concentration/temperature;
- V_x, V_y, V_z = Velocity vectors [m/s];
- α_L = Longitudinal dispersivity [m];
- α_T = Transversal dispersivity [m];
- V = Velocity [m/s];
- D_m = Molecular diffusivity [m^2/s];
- ϕ = Porosity;
- c_w = Concentration/temperature of injected water;
- Q = Pumping/injection rate [m^3/s],
- λ = Exponential decay constant [s^{-1}];

The retardation coefficient R_d is given by

$$R_d = 1 + \frac{\beta(1-\varphi)\rho_s}{\varphi\rho_1} \tag{15}$$

Here β is the retardation constant. For mass transport β is

$$\beta = K_d\rho_1$$

but for heat transport β is

$$\beta = \frac{C_s}{C_1}$$

and K_d = Distribution coefficient;
r_1 = Density of liquid [kg/m^3] (1000 kg/m$^{3)}$;
ρ_s = Density of porous medium [kg/m^3] (2500 kg/m^3);
C_1 = Specific heat capacity of liquid,
C_s = Specific heat capacity of porous medium.

Equation 14 is integrated vertically across each layer. The results are given below for *n* layers from top to bottom.

Top layer:

$$\frac{\partial}{\partial x}\left(\varphi b_1 D_{xx}\frac{\partial c_1}{\partial x}\right)+\frac{\partial}{\partial y}\left(\varphi b_1 D_{yy}\frac{\partial c_1}{\partial y}\right)-V_x b_1\frac{\partial c_1}{\partial x}-V_y b_1\frac{\partial c_1}{\partial y} = \varphi b_1 R_d\frac{\partial c_1}{\partial t}+\varphi b_1 R_d\lambda c_1-(c_o-c_1)R-Q(c_w-c_1)-\gamma_2(h_2-h_1)(c_{1,2}-c_1)-\delta_2(c_2-c_1) \quad (16)$$

Layer *i*:

$$\frac{\partial}{\partial x}\left(\varphi b_i D_{xx}\frac{\partial c_i}{\partial x}\right)+\frac{\partial}{\partial y}\left(\varphi b_i D_{yy}\frac{\partial c_i}{\partial y}\right)-V_x b_i\frac{\partial c_i}{\partial x}-V_y b_i\frac{\partial c_i}{\partial y} = \varphi b_i R_d\frac{\partial c_i}{\partial t}+\varphi b_i R_d\lambda c_i- Q(c_w-c_i)-\delta_i(c_{i-1}-c_i)-\delta_{i+1}(c_{i+1}-c_i)-\gamma_i(h_{i-1}-h_i)(c_{i,i-1}-c_i)-\gamma_{i+1}(h_{i+1}-h_i)(c_{i,i+1}-c_i) \quad (17)$$

Bottom layer:

$$\frac{\partial}{\partial x}\left(\varphi b_n D_{xx}\frac{\partial c_n}{\partial x}\right)+\frac{\partial}{\partial y}\left(\varphi b_n D_{yy}\frac{\partial c_n}{\partial y}\right)-V_x b_n\frac{\partial c_n}{\partial x}-V_y b_n\frac{\partial c_n}{\partial y} = \varphi b_n R_d\frac{\partial c_n}{\partial t}+\varphi b_n R_d\lambda c_n-Q(c_w-c_n)-\delta_n(c_{n-1}-c_n)-\gamma_n(h_{n-1}-h_n)(c_{n,n-1}-c_n) \quad (18)$$

where b_i = Saturated thickness of layer *i*; and
$c_{i,\,i+1}$ = c_i for outflow, and c_{i-1} for inflow.

Usually the parameters used in the transport part are not well known. Therefore the modeler needs to be careful when calibrating the model using real measured values of the contaminants.

3.2 Working with the flow and transport model

This section presents some hypothetical exercises. The main idea is to show how different conditions can affect the groundwater movement and the distribution of the contaminant plume, and also the importance of obtaining good information that helps to calibrate the model.

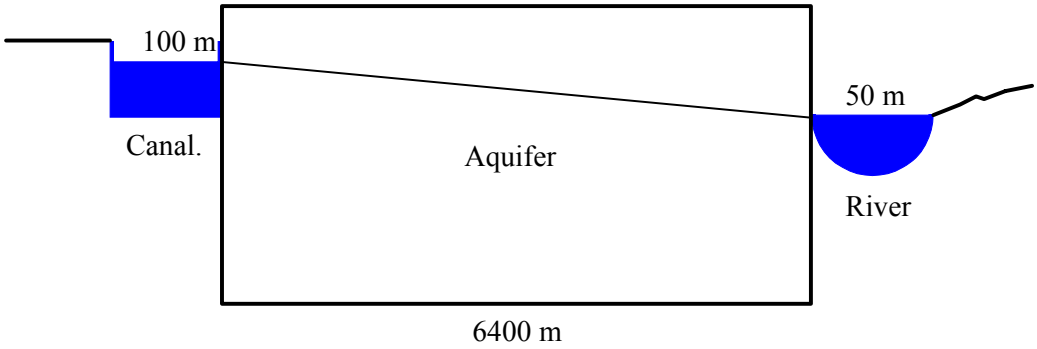

FIGURE 11: Vertical cross-section - case one

Case one:

Figure 11 shows a vertical cross-section through an unlined wastewater canal which is put into operation along one edge of an alluvial valley. Assuming that the canal and the river are fully penetrating, we want to calculate the contaminant concentration in the river. The following conditions are assumed:

Concentration of pollutant in the canal is 100 mg/l;
Infiltration in the area is 500 mm/year;
Transmissivity is 0.064 m^2/s;
Porosity is 0.3;
The aquifer thickness is 40 m; and
Longitudinal dispersivity is 50 m.

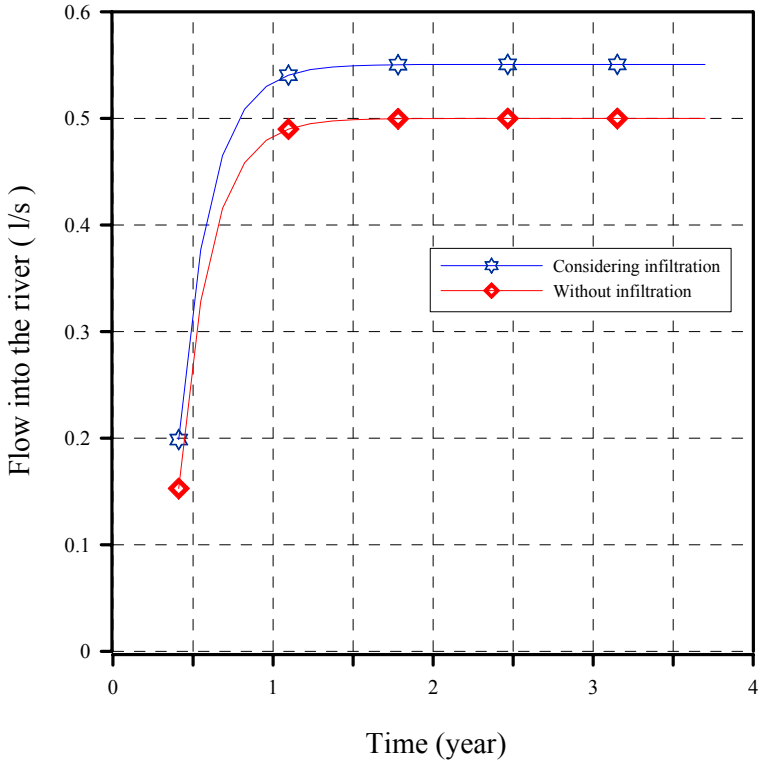

FIGURE 12: Flow reaching the river – case one

Figure 12 shows the result for the amount of water flowing into the river from the aquifer. Two different conditions are presented. In the first one, the effect of the head gradient between the canal and the river is taken into account leaving out the effect of infiltration. In this case the steady-state flow is 0.50 l/s into the river, as can be seen in Figure 12 (only 1 m length of the canal and river is modeled). In the second condition, the contribution of the infiltration into the aquifer is added. This results in 0.55 l/s flow into the river.

The model results can be easily checked doing some simple hand calculations. The amount of flow from the canal due to the head gradient is given by Equation 19:

$$q_H = K \times b \frac{h_c - h_r}{L} \tag{19}$$

where q_h = Flow coming into the river from the canal [l/s];
K = Permeability [m/s];
h_c = Head in canal [m];

h_r = Head in river [m];
b = Aquifer thickness [m];
L = Aquifer length.

With our present conditions Equation 19 gives

$$q_H = 0.0016 \times 40\,(100 - 50\,) / 6400 = 0.5 \text{ l/s}$$

The infiltration is calculated as follows:

$$Q_1 = R \times A \times Fc \qquad (20)$$

where q_I = Flow due to infiltration [l/s];
R = Infiltration rate [mm/year];
A = Area of contribution [m^2];
Fc = Factor to convert mm/year to m/s.

This gives

$$q_{in} = 0.5 + \tfrac{1}{2}\ 0.1 = 0.55 \text{ l/s}$$

$$q_I = 500 \times 1 \times 6400 \times 3.17 \times e^{-11} = 0.1 \text{ l/s}$$

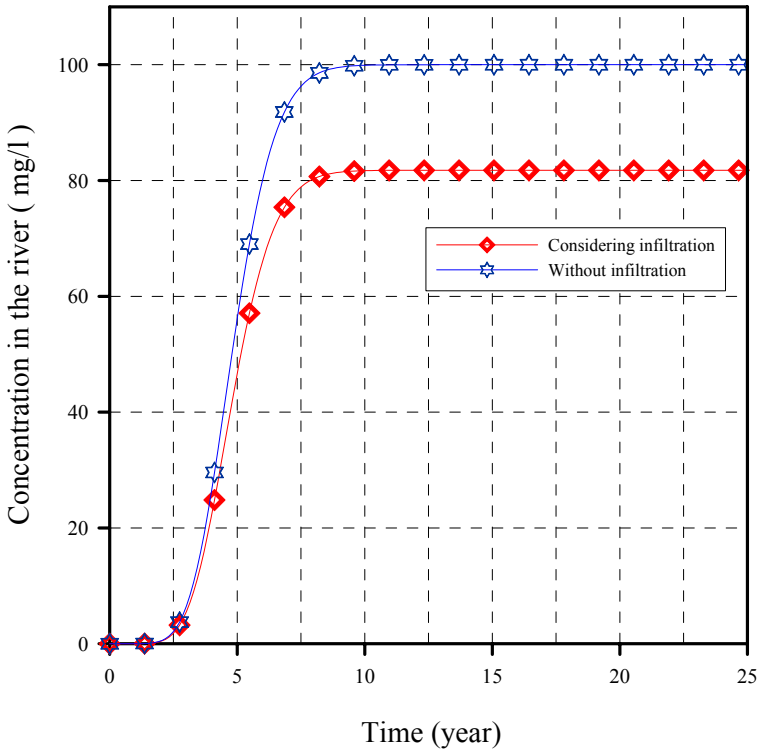

FIGURE 13: Concentration of contaminants reaching the river with time for case one

The total flow of the river is given by the sum of the flow from the head gradient and half the flow from the infiltration (law of superposition, the other half goes towards the canal).

Figure 13 shows the effect of infiltration on the concentration of pollutants in the river. When there is no infiltration over the model area, the concentration obtained in the river is 100 mg/l, the same as in the canal. Because there is no water to dilute the polluted water and decay, coefficients or retardation are not considered.

When the infiltration effect is considered, the concentration reaching the river is about 81.8 mg/l. Here the inflow provided by the infiltration dilutes the polluted water coming from the canal. Together with the condition used in the model this means that the infiltration of 500 mm/year reduces the pollution arriving to the river about 20%. Figure 13 shows that it takes the pollution about 750 days to reach the river, and approximately 3600 days to reach steady-state. As before, neither retardation nor decay is considered. This case does not consider molecular diffusion, retardation constants, decay of the pollutants, but they can be specified in the program. As for the flow model, this can be checked with simple calculations.

The mass balance can be written as

$$q_{out} \times c_o = q_{in} \times c \tag{21}$$

where q_{out} = The flow of the canal;
c_o = Initial concentration of pollutant;
q_{in} = The flow coming into the river from the canal plus infiltration.

Using the mass balance and the above simple calculations give

$$c = q_{out} / q_{in} \times 100 = 0.45 / 0.55 \times 100 = 81.8 \text{ mg/l}$$

which represents the concentration in the river in steady-state conditions, taking infiltration into account.

The breakthrough time, which is defined as the time for the concentration to reach the river, can be derived using Darcy's velocity

$$V = \frac{T}{b} \times \frac{(h - h_o)}{L} \tag{22}$$

which gives $V = (0.064 / 40) \times (100 - 50) / 6400 = 1.25 \times e^{-5}$ m/s

So the actual seepage velocity is

$$V = V / \varphi = 1.25 \times e^{-5} / 0.3 = 4.17 \ e^{-5} \text{ m/s}$$

This gives the breakthrough time

$$t_b = L / V_a = 6400 / 4.17 \ e^{-5} = 1778 \text{ days}$$

The result can be compared with the time in Figure 13 corresponding to the mid-concentration value of 40.9 mg/l. The concentration in the river calculated by the model after 1778 days is 42 mg/l. The difference is due to dispersion effects that the simple calculations do not take into account.

Case two:
We will consider a hypothetical situation where we wish to predict the effect of a waste disposal site on an abstraction borhole. We assume that the catchment area is rectangular, 2000x500 m, as shown in Figure 14. The following parameters are used:

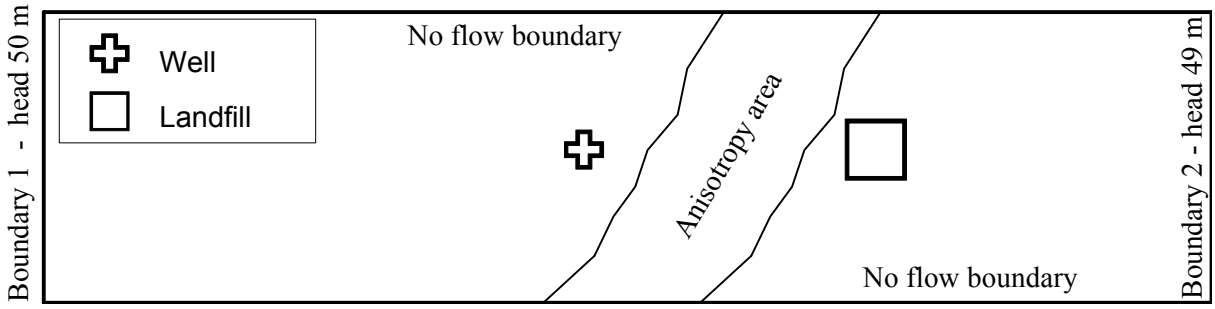

FIGURE 14: Model area - case two

The average concentration in the infiltrated water through the landfill is 30 mg/m^3;
Pumping of 0.04 m^3/s from layer 3;
The top layer is 10 m deep, the second and the bottom layer are 20 m deep;

Longitudinal dispersivity is	50 m;
Transversal dispersivity is	5 m;
Porosity is	0.1;
Vertical permeability in the landfill is	2×10^{-9} m/s;
Vertical permeability in the other area is	2×10^{-6};
Horizontal permeability in the landfill is	2×10^{-9};
Horizontal permeability in the other area is	2×10^{-4}.

The boundary conditions are 50 m head on the left-hand side and 49 m on the right-hand side boundaries and the infiltration over the whole area is 500 mm/year.

In Figure 15, the calculated results are shown using the above mentioned parameters, of the groundwater flow and the contamination plume for all three layers. For each layer are two sets of figures, the upper one without the pumping of the well, and the lower one including the effect of pumping.

When there is no pumping, the flow in all the layers is going from the left hand side (higher head) to the right hand side (lower head) and is similar in all layers. Close to the landfill in the top and middle layer, there is a small change in the flow direction. This is because of different permeability in the landfill than elsewhere in the aquifer. Under these conditions the flow is moving the plume toward the right-hand boundary and the major pollution is in the area at the right side

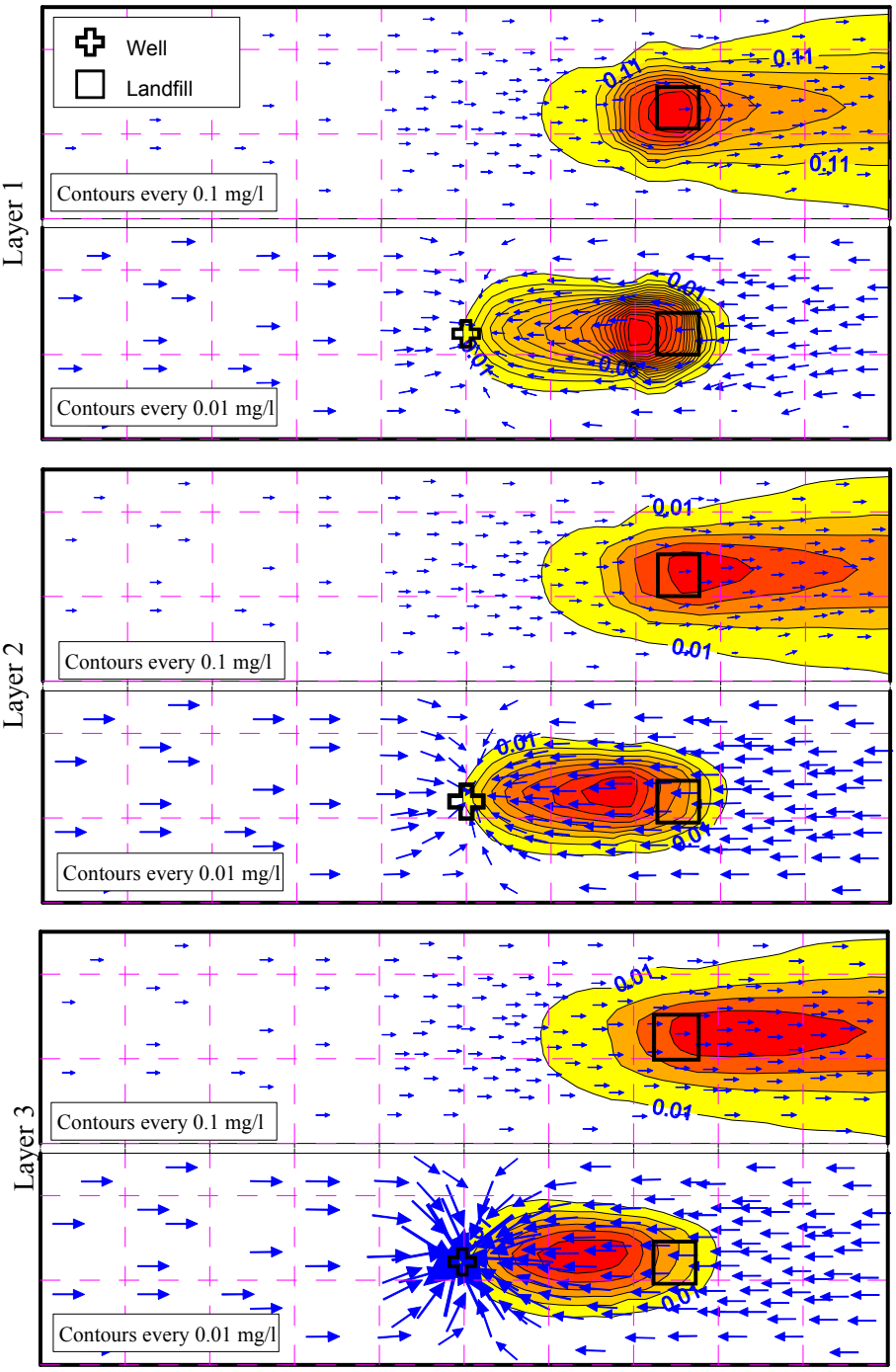

FIGURE 15: Flow and dispersion plume in different layers - case two

of the landfill. Due to dispersion, the area to the left of the landfill gets contaminated, showing that pollution can travel in the opposite direction of flow. The distribution of the plume perpendicular to the flow direction is also due transversal dispersion. The greater the transversal distribution is, the more distributed the plume is in the direction perpendicular to flow direction. The lower figure for each layer in Figure 15 represents the second state where there is a well pumping from the bottom layer.

The effect of pumping on the flow field is clear in the figures. It is greater in layers two and three than in the top layer, because the pumped water stands higher than the contribution of the infiltration. The flow is completely reversed and water now flows in from both sides. The contaminant plume is also inverted and is now forward of the landfill to the well zone like the flow. The plume distribution is smaller that in the first case and its extension through the right hand side of the landfill is less. This is because groundwater velocity affects the distribution of the plume and now the flow in the system is faster due the flow demand from the well.

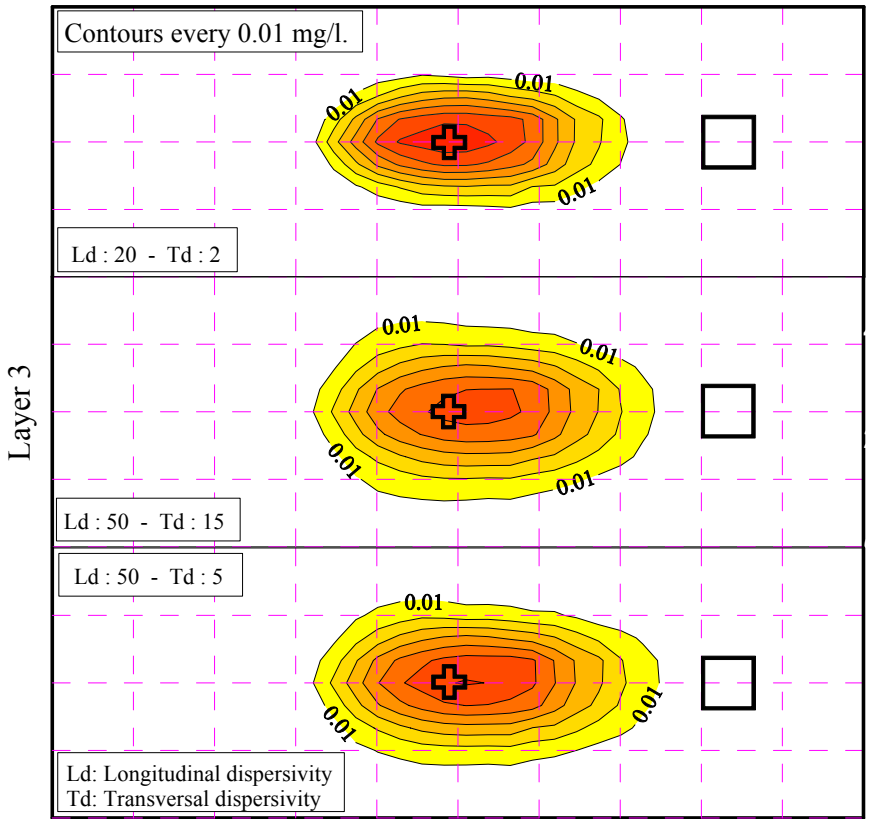

FIGURE 16: Effects of dispersivity in plume distribution – case two

Figure 16 shows the effect of changed dispersivity in the above model (with pumping). The longitudinal dispersivity (a_L) was changed from 50 to 20 m and the transversal one from 5 to 2 m. The effect is a narrower plume when the transversal dispersion is decreased. The effect of changing the longitudinal dispersivity is not so great. This is because higher values of a_t result in the pollution moving more easily in a direction perpendicular to the flow.

Figure 17 shows the effect of changes in the values of anisotropy, representing a fissure between the well and the landfill, as is shown in Figure 14. In this scenario the fissure is either at an angle of 45 or 90 degrees, and permeability along the fissure is 20 times greater than perpendicular to it. As can be seen, the effect of the fissure is great both on the flow and the plume. This underlines the importance of knowing the geology in the model area well, and simulating different scenarios.

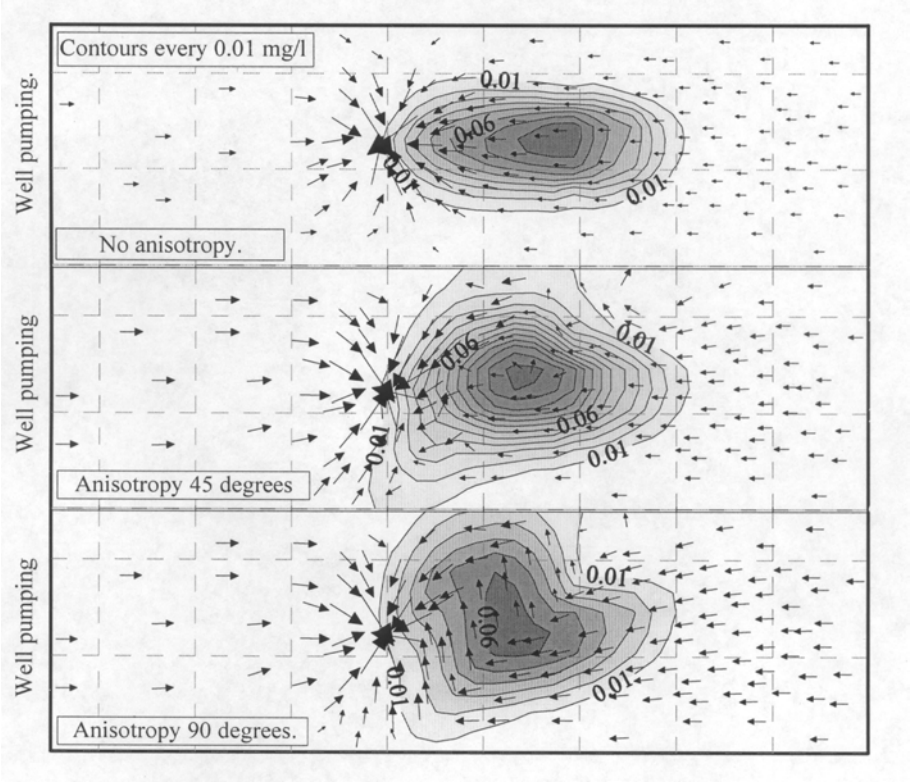

FIGURE 17: Effects of anisotropy in the plume dispersion and groundwater flow - case two

Case 3

The aquifer is three layers with the characteristics given in Table 5.

TABLE 5: Characteristics of the three layered aquifer given in case 3

Description / Layer	**Top**	**Middle**	**Bottom**
Thickness [m]	32	18	50
Horizontal permeability [m/s]	10×10^{-8}	10×10^{-4}	10×10^{-3}
Vertical permeability [m/s]	10×10^{-8}	10×10^{-6}	10×10^{-5}
Specific storage coefficient [m^{-1}]	10×10^{-4}	5×10^{-6}	2×10^{-6}
Porosity	0.1	0.1	0.1
Longitudinal dispersivity [m]	50	50	50
Vertical dispersivity [m]	5	5	5

In the third case the size of the model area is 5000 × 2000 m. Centred in the co-ordinates (600, 100) there is a lagoon containing wastewater which is constantly leaking. It is known that the concentration of the leaking water is 60 mg/l. The leak is 0.00014 m^3/s. The infiltration rate over the whole area is 109.5 mm/year. In the model area there is a river as shown in Figure 18. The general flow is from left to right because of the gradients. Three scenarios are studied:

1. The model is calculated for only the river and the lagoon present in the area and no pumping.
2. One well for extracting fresh water from layer 3 at the rate of 0.01 m^3/s is added at coordinates (4000, 667). The well starts pumping at 4000 days.
3. Finally, 800 days after beginning pumping from the first well, another is added at the coordinates (3000, 1667) pumping, from layer 2 at the rate of 0.02 m^3/s.

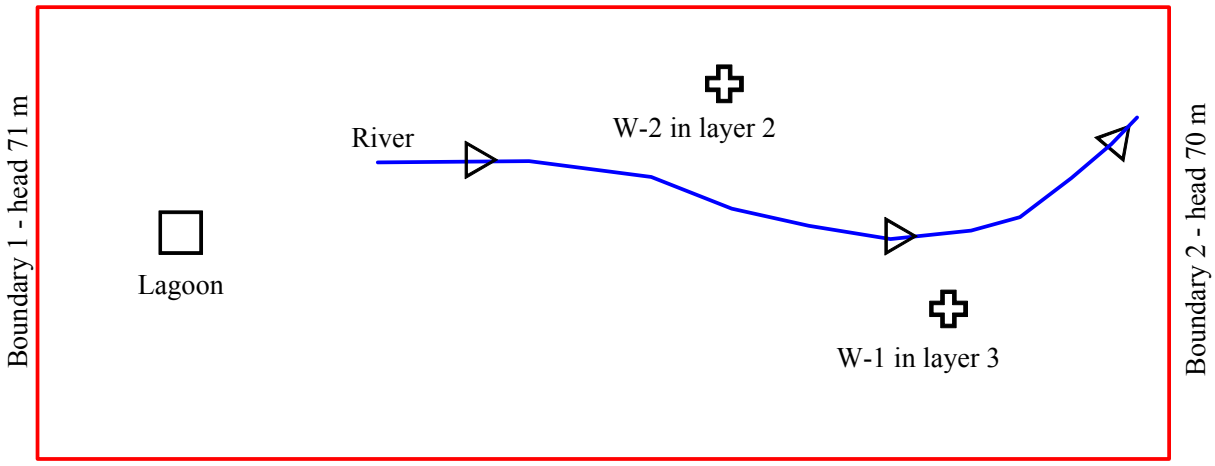

FIGURE 18: Model area – case three

The model is calculated for 8000 days or about 22 years, which is considered the life of the geothermal project. Figure 19 shows that the effect of the wells on the river flow is negligible.

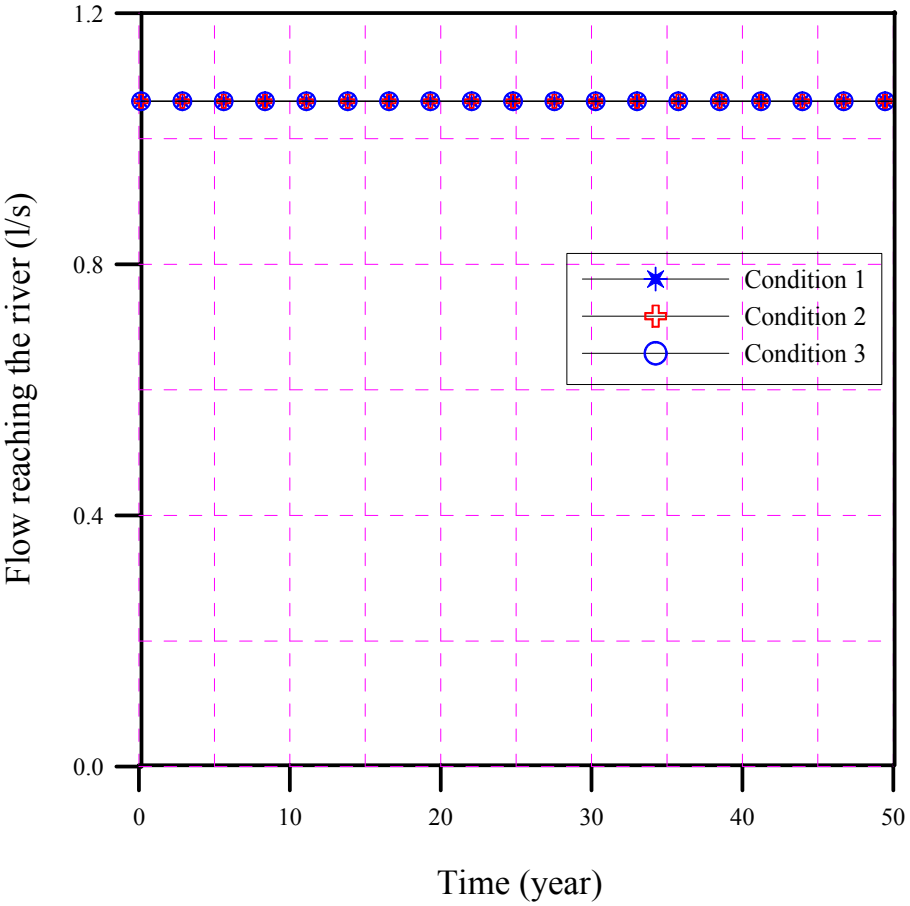

FIGURE 19: Flow reaching the river – case three

The wells affect the contamination in the river as shown in Figure 20. When pumping starts, the contamination in the river is reduced. As seen from the figure, contamination reaches the river at approximately 8000 days, when the lifetime of the project is over. For scenario one, the maximum concentration reaching the river is 0.0230 mg/l after 69 years, for scenario two 0.0201 mg/l after 63 years and for scenario three 0.0173 mg/l after 47 years. After that, the concentration decreases. To completely clean the pollution reaching the river, the hydrological system needs at least 164 years for scenario three and more than 190 years in the other cases, but of course this depends on the parameters used.

Figure 21 shows the values of contaminant in the wells. When only the well in the bottom layer is present the maximum concentration is 0.164 mg/l 55 years after the project is over. In scenario three where two wells are present, the concentration in well No.1 is 0.009 mg/l and in well No. 2 in the middle layer it is 0.23 mg/l after 59 years. The water in well No. 2 in layer two is more contaminated than in the other well because of higher abstraction and the fact that it is closer to the lagoon than the well in layer three.

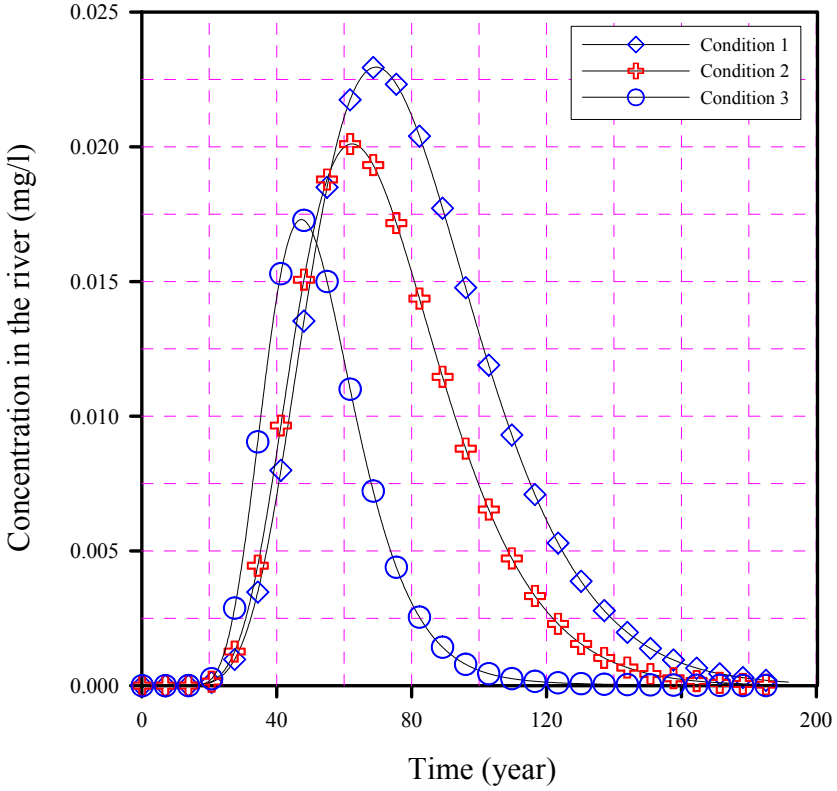

FIGURE 20: Concentration of contaminants reaching the river for different scenarios

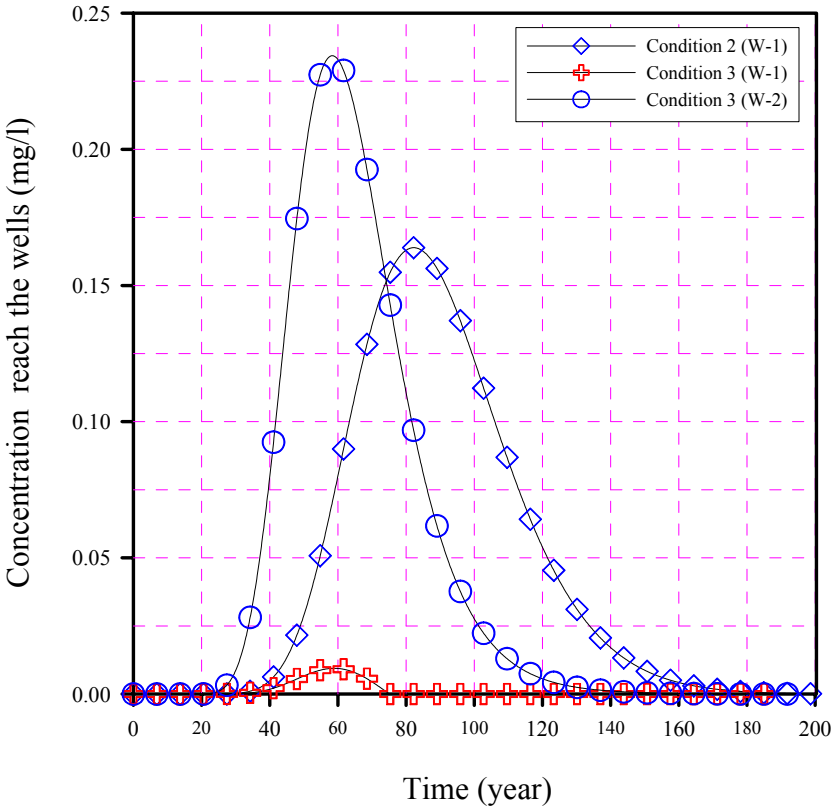

FIGURE 21: Concentration of contaminants reaching the wells for different scenarios

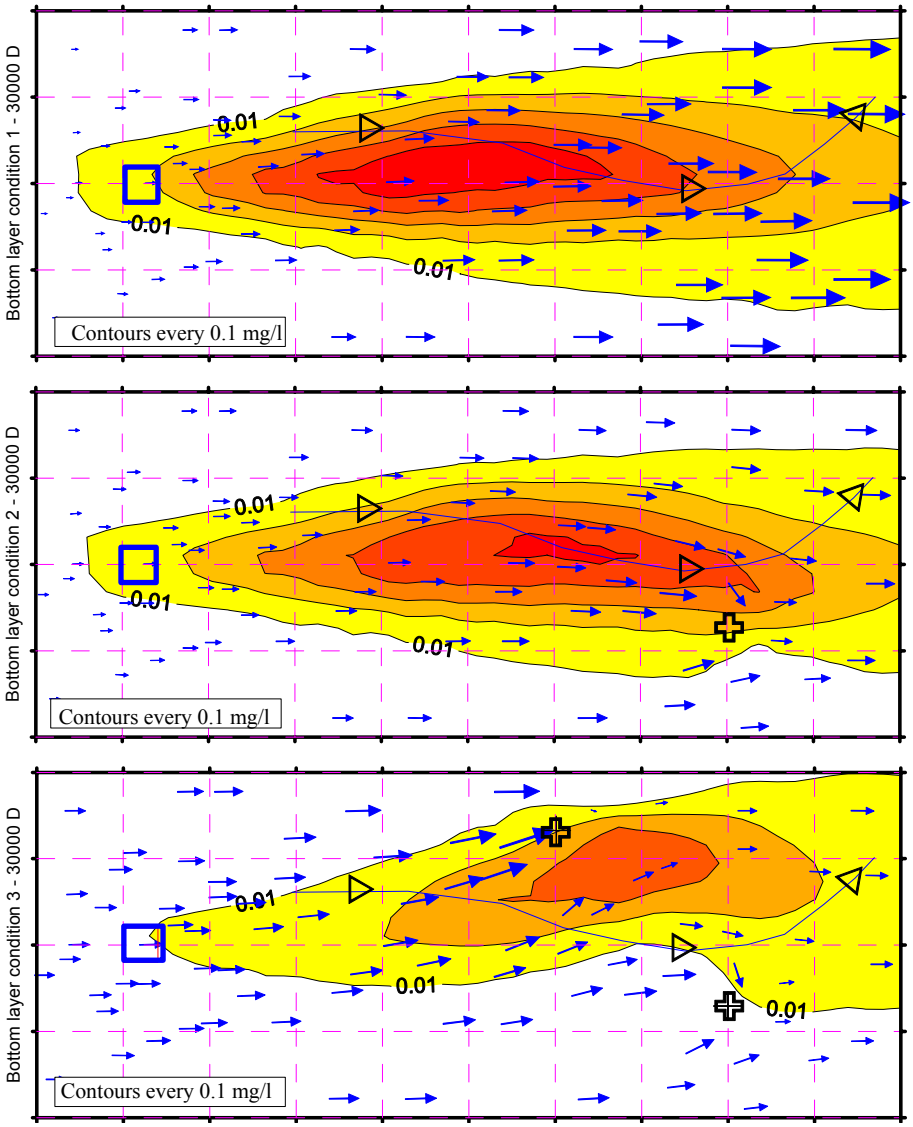

FIGURE 22: Plume dispersion and groundwater flow direction for different scenarios in layer three

The changes in flow and concentrations due to the different conditions present in the area, also affect plume distribution. In Figure 22 the distribution plumes in the bottom layer are presented. The Figure shows the status after 82 years, the time for maximum concentration in well No. 1. In condition one (no wells in the area), the plume distribution is more or less symmetric along the X-axis across the middle of the lagoon, widening while moving to the right. This is because the general flow is moving to the right side and the effect of the dispersivity widens the plume. The status in condition two, when the well is pumping from layer three, is similar in the beginning but the plume distribution changes up close to the well. The well abstraction reduces the plume width. Pumping from the well moves the plume faster toward the right-hand side boundary. The values for the maximum concentrations now are further away from the lagoon than they were at the same time for no pumping.

In condition three, with both wells pumping, the situation is also similar but the rate for the well in layer two is twice as big as for the the well in layer three. That produces major flow demand from well No. 2. Now the abstraction is three times higher and the maximum concentration of the plume is moved towards the area between the wells.

4. CONCLUSIONS AND RECOMMENDATIONS

4.1 Conclusions for the Miravalles H_2S dispersion modeling

- The H_2S emissions from the Miravalles power plants do not represent problems for the environment or human health, and concentrations stay below the maximum allowed limits.
- The added emission when Miravalles III starts will not lead to important changes in the actual H_2S concentrations.
- The only town where the H_2S concentrations might reach more than 42 g/m3 is Cuipilapa.
- It is necessary to make measurements to determine the real H_2S concentrations at different meteorological conditions and then calibrate the model to confirm the model calculations.

4.2 Conclusions for the groundwater flow and transport of contaminants model

- It demonstrates how the AQUA3D program can be used to predict groundwater contamination. Due to the extremely complex groundwater movement, a good knowledge of the hydro-geology is necessary.
- The influence of particular conditions like wells, river, springs and others in the model area, over the dispersal of pollutants was also demonstrated.
- Monitoring within the project areas must be done over long periods of time, because the transport processes change more slowly than the flow processes.
- Groundwater models can be used as an aid in deciding where best to monitor possible contamination.

4.3 Recommendations

- It is necessary to collect meteorological data for some years and make simulations every month to compare the dispersion rate for different weather conditions.
- It is necessary to construct an active H_2S monitoring station network to calibrate the H_2S dispersion model.
- It is necessary to do research on hydro-geological data before setting up the groundwater flow and transport model for the Miravalles geothermal field.

ACKNOWLEDGEMENTS

Primarily I would like to express my gratitude to God because without his help and support I never could do anything. I am thankful to my wife Yesenia and my daughter Kendry for their patient, comprehension and unconditional support. Hearty gratitude to my parents Enue Sequeira and Victor Guido. Special thanks to the United Nations University and the Icelandic government for allowing me to take part in the geothermal training. I am grateful to my main advisor Sigurdur Lárus Hólm for his help with my project, Halldór Ármannsson for co-ordinating the environmental impact training and Jóhanna Thorlacius at the Meterological office for her help. Thank you, Dr Ingvar Fridleifsson and Lúdvík Georgsson for guidance during training, and Gudrún Bjarnadóttir for your efficient and always unconditional assistance.

Also, I would like to express my thanks to Dr. Alfredo Mainieri and Lic. Antonio Yock in Costa Rica for giving me the opportunity to take part in this training. To my friends, Eddy Sánchez and Osvaldo Vallejos, for their help and assistance and to Mr. Gerardo Campos for his counsel and good wishes to me. Thanks a lot. God bless all of you.

REFERENCES

Ármannsson, H., and Kristmannsdóttir, H., 1992: Geothermal environmental impact. *Geothermics, 21-5/6,* 869-880.

Armstead, H.C., 1983: *Geothermal Energy*. J.W. Arrowsmith Ltd., Bristol (2nd edition), 404 pp.

Bogarín C., R., 1996: Geothermal gases as a source of commercial CO_2 in Miravalles, Costa Rica and Haedarendi, Iceland. Report 3 in: *Geothermal Training in Iceland 1996*. UNU G.T.P., Iceland, 23-44.

Brown, K.L., 1995: Occupational safety and health. In: Brown, K.L. (convenor), *Environmental aspects of geothermal development*. World Geothermal Congress 1995, IGA pre-congress course, Pisa, Italy, May 1995, 3-37.

California Air Resources Board., 1999: *Ambient air quality standards*. CARB, Internet Website (http://www.arb.ca.gov/ags/aags2.pdf), USA.

EPA, 1999: *Air Pollution*. EPA Internet Website (http://www.epa.gov/ttn/uatw/3_90_024.htm), USA.

ICE, 1996: *Miravalles, environmental impact assessment of the 3rd and 4th unit*. Instituto Costarricense de Electricidad and Electroconsult, report ELC GMV-2-ELC-R-12535 (R01) (in Spanish), Costa Rica.

ICE 1988: *Miravalles, environmental impact assessment.* Instituto Costarricense de Electricidad, report (in Spanish), Costa Rica.

Reed, M.J., and Renner, J.L., 1995: Environmental compatibility of geothermal energy. In: Frances, S.S. (editor), *Alternative fuel and the environment*. Lewis, Florida, USA, 23-37.

Trinity Consultants, 1999: *User guide for the BREEZE HAZ SUITE*. Trinity Consultants, USA, 206 pp.

Vallejos, O., 1996: A conceptual reservoir model and numerical simulation studies for the Miravalles Geothermal field, Costa Rica. Report 18 in: *Geothermal Training in Iceland 1996.* UNU G.T.P., Iceland, 419-456.

Vatnaskil, 1998a: *Groundwater flow and contaminant transport model - user's manual*. Vatnaskil Consulting Engineers, Iceland, 69 pp.

Vatnaskil, 1998b: *Groundwater flow and contaminant transport model*. Vatnaskil Consulting Engineers, Iceland, 86 pp.

WHO, 1999a: "*Climate and Health"*. Internet Website (http://www.who.int/peh/climate/climate_and_health.htm) World Health Organization, 1999.

World Health Organization, 1999b: "*Air quality"*. Internet Website (http://www.who.int/peh/air/airindex.htm) World Health Organization, 1999.